



Since January 2020 Elsevier has created a COVID-19 resource centre with free information in English and Mandarin on the novel coronavirus COVID-19. The COVID-19 resource centre is hosted on Elsevier Connect, the company's public news and information website.

Elsevier hereby grants permission to make all its COVID-19-related research that is available on the COVID-19 resource centre - including this research content - immediately available in PubMed Central and other publicly funded repositories, such as the WHO COVID database with rights for unrestricted research re-use and analyses in any form or by any means with acknowledgement of the original source. These permissions are granted for free by Elsevier for as long as the COVID-19 resource centre remains active.

Role of endocytosis and cathepsin-mediated activation in Nipah virus entry

Sandra Diederich, Lena Thiel, Andrea Maisner*

Institute of Virology, Philipps University of Marburg, Germany

Received 18 October 2007; returned to author for revision 7 December 2007; accepted 8 February 2008

Available online 14 March 2008

Abstract

The recent discovery that the Nipah virus (NiV) fusion protein (F) is activated by endosomal cathepsin L raised the question if NiV utilize pH- and protease-dependent mechanisms of entry. We show here that the NiV receptor ephrin B2, virus-like particles and infectious NiV are internalized from the cell surface. However, endocytosis, acidic pH and cathepsin-mediated cleavage are not necessary for the initiation of infection of new host cells. Our data clearly demonstrate that proteolytic activation of the NiV F protein is required before incorporation into budding virions but not after virus entry.

© 2008 Elsevier Inc. All rights reserved.

Keywords: Nipah virus; Endocytosis; Cathepsin cleavage; Virus entry

Introduction

The highly pathogenic Nipah virus (NiV) was isolated in 1999 after an outbreak of fatal encephalitis among pig farmers in Malaysia and Singapore (Chua, 2003). Old World fruit bats of the genus *Pteropus* have been identified as the natural host of NiV (Yob et al., 2001). Because of several unique genetic and biological characteristics NiV and the closely related Hendra virus form the new genus *Henipavirus* within the *Paramyxoviridae* family (Harcourt et al., 2000; Wang et al., 2000). Due to their broad host range and the high mortality rates associated with infection, the henipaviruses have been classified as Biosafety Level 4 (BSL4) agents.

As most paramyxoviruses, NiV encodes for two surface glycoproteins which are essentially required for the virus entry process. After binding of the G protein to the cellular surface receptor, the fusion protein F mediates fusion of the viral and cellular membranes. Recently, ephrin B2 (EB2) has been shown to function as main entry receptor for NiV (Bonaparte et al., 2005; Negrete et al., 2005). EB2 is a transmembrane-anchored ligand of the receptor tyrosine kinases EphB2, EphB3 and EphB4, and plays a critical role in embryonic patterning, axon guidance and angiogenesis (Adams, 2002; Kullander and Klein,

2002). As EB2 is predominantly expressed on endothelial cells and neurons (Adams, 2002), this is consistent with the known cellular tropism for NiV (Wong et al., 2002).

For successful virus entry into EB2-expressing cells, a fusion-active NiV F protein is required. As other paramyxoviral F proteins, the NiV F protein is synthesized as inactive precursor and is cleaved by host cell proteases into the subunits F₁ and F₂. Thereby the hydrophobic fusion peptide at the N-terminus of F₁ is released. Interestingly, the recently uncovered proteolytic cleavage mechanism used by henipavirus F proteins differs fundamentally from that utilized by related viruses. Other paramyxoviral fusion proteins are either processed by extracellular trypsin-like proteases after reaching the cell surface or after being incorporated into budding viruses, or they are cleaved by the Golgi protease furin during transport along the secretory pathway (Klenk and Garten, 1994). Because most of the F proteins in virus particles are cleaved and fully fusion competent, paramyxoviruses can enter new host cells via fusion of the viral membrane and the plasma membrane at neutral pH (Earp et al., 2005). However, henipavirus F proteins are neither cleaved by trypsin- nor furin-like proteases but must be activated by cathepsin L (CTSL) within an acidic endosomal compartment (Diederich et al., 2005; Meulendyke et al., 2005; Pager and Dutch, 2005; Pager et al., 2006). Cleavage efficiency strongly depends on endocytic activity and the expression level of CTSL which varies markedly in different cell types. Even though some cleaved F protein is expressed on the surface of all cells tested so far, the

* Corresponding author. Institut für Virologie, Hans-Meerwein-Str. 2, D-35043 Marburg, Germany. Fax: +49 6421 2868962.

E-mail address: maisner@staff.uni-marburg.de (A. Maisner).

percentage of cleaved NiV F protein is generally low (Moll et al., 2004a; Diederich, unpublished). Thus, most of the F protein present on the plasma membrane is not fusion competent. This raised the question if NiV particles released from infected cells contain sufficient amounts of activated F protein to enter a new host cell directly by pH-independent fusion with the plasma membrane, or if virus endocytosis and subsequent F cleavage by endosomal CTSL are essential for the entry process. The aim of this study was to clearly define which steps of the NiV replication cycle require endocytic and proteolytic processes.

Results

The NiV receptor EB2 is endocytosed in different cell types

The idea of NiV entry via receptor-mediated endocytosis was supported by the recent report that the NiV receptor EB2 is internalized from human endothelial cells (Korff et al., 2006). To analyze if EB2 endocytosis is a general phenomenon in NiV-susceptible cells, we performed a qualitative uptake assay using Vero, MDCK, PAEC or HeLa cells which have been transfected with an EB2-encoding expression plasmid. After addition of recombinant mouse EphB4/Fc, a soluble EB2 receptor fused to the Fc region of human IgG, cells were incubated at 37 °C for 1 h to allow binding of EphB4 and co-endocytosis of EB2 and EphB4/Fc. Surface-remained EphB4/Fc was then stained with a rhodamine-conjugated secondary antibody at 4 °C. After permeabilization, internalized EphB4/Fc was visualized by incubation with a FITC-conjugated secondary antibody. Fig. 1 clearly shows that numerous fluorescent intracellular vesicles (green) were found in all EB2-expressing cells indicating that the EB2 receptor is efficiently endocytosed in NiV-susceptible cells.

G-containing VLPs and NiV particles are internalized from the surface of EB2-expressing cells

To determine if NiV particles bound to EB2-expressing cells are also internalized, we made use of the recent finding that the NiV G protein is released in virus-like particles (VLPs) upon single expression (Patch et al., 2007). The G-containing VLPs resemble infectious NiV particles in shape and size (not shown) and can therefore be utilized to study G-mediated attachment and uptake into host cells outside of the BSL4 facility. VLPs were generated by transfection of 293T cells with the NiV G_{tag} gene. At 72 h post transfection, supernatants were clarified by low-speed centrifugation and pelleted through a 20% sucrose cushion. VLP-containing pellets were resuspended and added to EB2-expressing cells in combination with an antibody directed against the HA-tag. After 1 h at either 4 °C or 37 °C, surface-bound antibodies were stained with a FITC-conjugated secondary antibody at 4 °C. After permeabilization, internalized VLPs were visualized with a rhodamine-conjugated secondary antibody and cell nuclei were counterstained with DAPI. Merged pictures of the FITC, rhodamine and DAPI fluorescence channels are shown in Fig. 2A. As expected, no intracellular VLPs could be detected in the sample incubated at 4 °C (Fig. 2A,

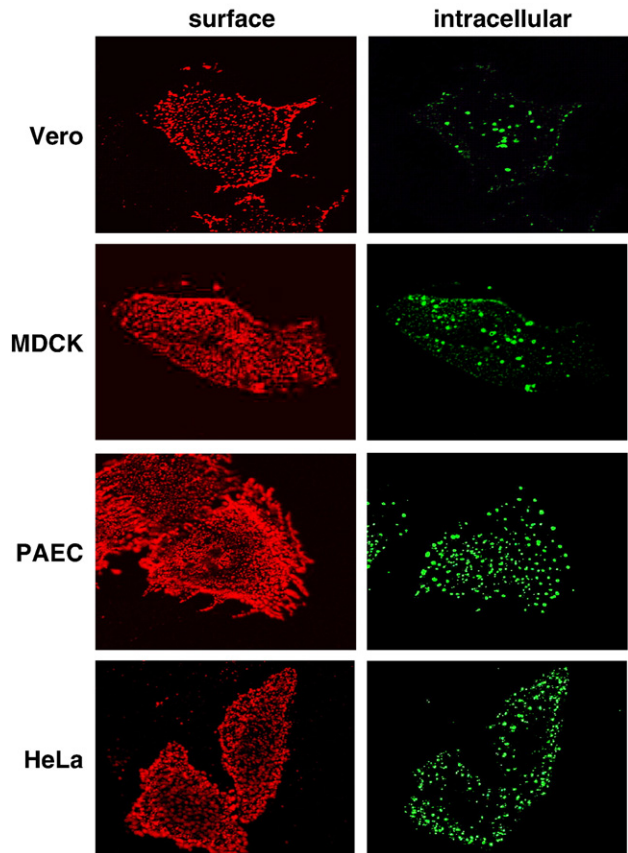


Fig. 1. Endocytosis of EB2 in different cell lines. EB2-expressing cells (Vero, MDCK, PAEC, and HeLa) were incubated with EphB4/Fc for 1 h at 37 °C to allow binding and endocytosis to proceed. Surface-remained EphB4/Fc was stained with a rhodamine-conjugated anti-human IgG antibody (surface). After fixation and permeabilization, internalized EphB4/Fc was detected by a FITC-conjugated secondary antibody (intracellular).

control-4 °C). In contrast, a substantial amount of VLPs was found within the cells (red dots) if endocytosis was allowed at 37 °C (Fig. 2A, control-37 °C). When we performed the VLP uptake assay in the presence of 0.45 M sucrose which is known to inhibit endocytic uptake in general, internalization was clearly inhibited (Fig. 2B, + sucrose). Many VLPs had bound to the surface of sucrose-treated cells (green dots), but intracellular VLPs were found less frequently. In order to reveal the endocytic pathway required for VLP uptake, either 25 μM chlorpromazine, an inhibitor of clathrin-dependent internalization, or 5 mM β-methyl-cyclodextrin (MCD), an inhibitor of caveolae-dependent endocytosis, was added prior and during uptake of the VLPs. Chlorpromazine had basically no negative effect on the internalization indicating that clathrin-mediated endocytosis is not involved (Fig. 2B, + chlorpromazine). In contrast, MCD which removes membrane cholesterol and disrupts lipid rafts thereby preventing uptake via caveolae, markedly inhibited VLP endocytosis (Fig. 2B, + MCD). To quantify the effect of the inhibitors on VLP uptake, the number of internalized VLPs in 40 randomly chosen cells of each sample was counted and averaged. When VLP uptake in untreated cells incubated at 37 °C (Fig. 2B, control-37 °C) was set at 100%, chlorpromazine inhibited

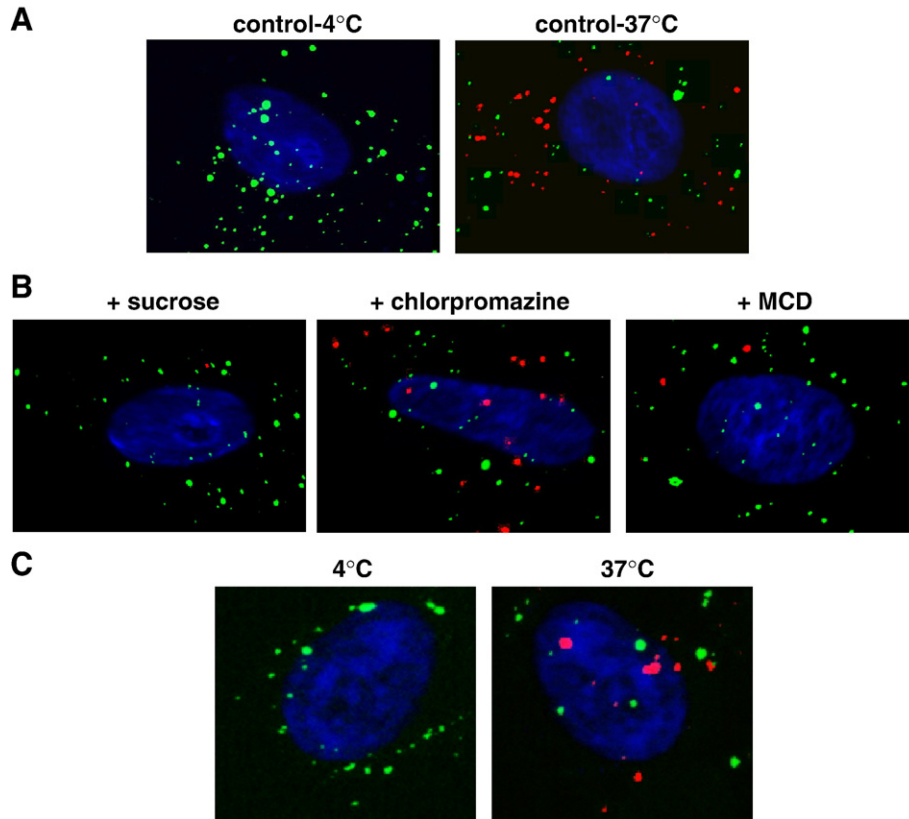


Fig. 2. VLP- and virus-uptake assays. (A) Vero cells were incubated for 1 h at 4 °C (control-4 °C) or at 37 °C (control-37 °C) with purified NiV G_{tag}-containing VLPs in combination with a monoclonal antibody directed against the HA-tag. Surface-bound VLPs were visualized by incubation with FITC-conjugated anti-mouse IgG antibodies at 4 °C. After permeabilization with methanol–acetone, intracellular VLPs were stained with a rhodamine-conjugated secondary antibody. Nuclei were visualized by DAPI staining. Merged pictures of the DAPI, FITC and rhodamine fluorescence channels are shown. (B) Cells were preincubated for 30 min at 37 °C with the following endocytosis inhibitors: 0.45 M sucrose (sucrose), 25 μM chlorpromazine (chlorpromazine) or 5 mM β-methyl-cyclodextrin (MCD). Incubation with VLPs and HA-tag antibody was performed for 1 h at 37 °C in the presence or absence of the inhibitors. Surface-bound and intracellular VLPs were stained as described above. (C) Vero cells were incubated with infectious NiV particles for 2 h at 4 °C. After incubation with anti-NiV serum for 30 min on ice, cells were either shifted to 37 °C or kept at 4 °C for 20 min. Surface-bound and intracellular antibodies were visualized as described above.

endocytosis by only 11%, whereas sucrose and MCD treatment produced a 48% and 51% uptake inhibition, respectively. This result suggests that internalized VLPs have entered the cells via caveosomes. In agreement, internalization of EB2 was also significantly reduced in the presence of sucrose and MCD (data not shown).

To support the idea of endocytic particle uptake, we performed an uptake assay using infectious NiV. For this, NiV particles were concentrated and partially purified from infected cell supernatants. Viruses were then adsorbed to Vero cells and labeled with an anti-NiV serum at 4 °C. Subsequently, cells were either shifted to 37 °C to allow endocytosis of surface-bound virions, or were kept at 4 °C. Antibodies on the cell surface were then detected by FITC-conjugated secondary antibodies and internalized virus–antibody complexes were stained with rhodamine-coupled secondary antibodies after cell permeabilization. If cells were not shifted to 37 °C, no intracellular staining was observed (Fig. 2C, 4 °C), but numerous intracellular (red) viruses could be detected after incubation at 37 °C when uptake of virus particles was allowed (Fig. 2C, 37 °C). This demonstrates that a substantial portion of surface-bound NiV particles can enter the cells via endocytosis. Together, these findings supported the concept that NiV uptake by receptor-

mediated endocytosis might be an additional or alternative route of virus entry to fusion at the plasma membrane.

Endocytosis and cathepsin inhibitors efficiently prevent NiV F protein cleavage

In order to investigate the efficacy of various drugs and inhibitors to interfere with NiV F cleavage in Vero cells, substances

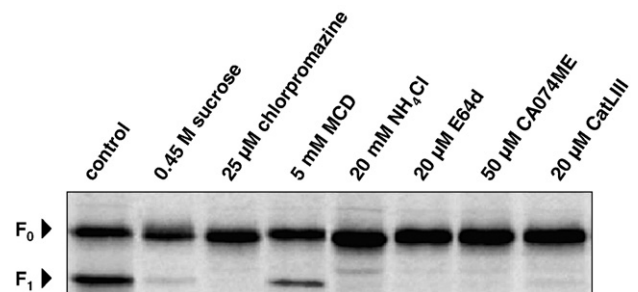


Fig. 3. Effect of endocytosis inhibitors, NH₄Cl, and cathepsin inhibitors on F protein cleavage. Vero cells expressing the NiV F protein were radiolabeled with [³⁵S]-Promix for 10 min and were then incubated in chase medium containing the indicated inhibitors for 2 h. F proteins were immunoprecipitated from cell lysates, separated on a 12% SDS gel under reducing conditions, and subjected to autoradiography.

either affecting endocytosis (sucrose, chlorpromazine, MCD), or preventing acidification of the endosome (NH_4Cl) or inhibiting CTSL-mediated cleavage (E64d, CatLIII, CA074ME), were assayed for their inhibitory effects on F protein cleavage. Here, F-transfected Vero cells were metabolically labeled with [^{35}S]-cysteine and -methionine for 10 min and incubated for 2 h in the absence or presence of different concentrations of the various inhibitors. After cell lysis, F proteins were immunoprecipitated, separated on a 12% SDS gel under reducing conditions, and subjected to autoradiography. In Fig. 3, the results are shown for the optimal inhibitor concentrations, thus the highest drug con-

centrations showing no cytotoxic effect within 2 h. Non-specific inhibition of all endocytic processes by 0.45 M sucrose as well as specific inhibition of clathrin-mediated endocytosis by 25 μM chlorpromazine almost completely prevented proteolytic processing of F_0 into F_1 and F_2 . This confirms our previous findings in MDCK cells that F cleavage depends on a tyrosine-dependent motif in the cytoplasmic tail which mediates endocytosis via clathrin-coated pits (Diederich et al; 2005). In contrast to chlorpromazine treatment, addition of MCD only slightly affected F protein processing (Fig. 3, 5 mM MCD). This demonstrates that caveolae-mediated endocytosis is not predominantly involved in

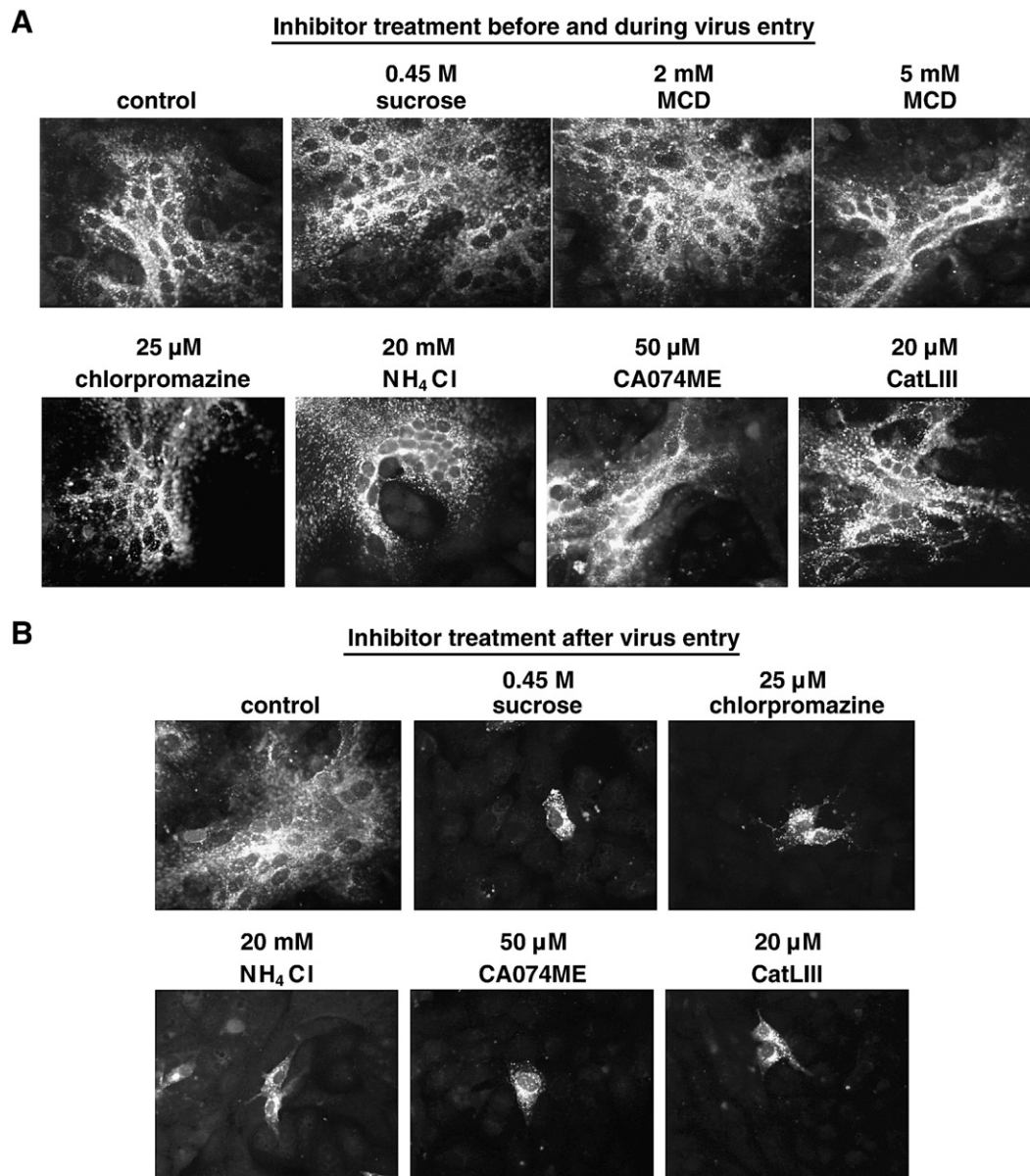


Fig. 4. Effect of inhibitor treatments during and after virus entry on NiV infection. (A) Inhibitor treatment before and during virus entry. Vero cells were infected with NiV at a MOI of 0.2. Cells were treated with the indicated inhibitors for 1 h prior infection and for 1 h at 37 °C during virus adsorption and entry, or were left untreated (control). Then, inhibitors and input virus were removed, cells were washed and further incubated in medium for 24 h at 37 °C. After fixation and permeabilization, cells were incubated for 1 h on ice with a polyclonal anti-NiV serum and primary antibodies were detected with rhodamine-conjugated secondary antibodies. (B) Inhibitor treatment after virus entry. After infection of Vero cells with NiV for 1 h at 37 °C, cells were washed and then incubated in the absence (control) or presence of the indicated inhibitors. At 24 h p.i., immunostaining was performed as described above. There was no generalized toxicity effect of any of the inhibitors at the concentrations used in this experiment.

Table 1
Effect of endocytosis inhibitors, NH_4Cl , and cathepsin inhibitors on the production of infectious NiV

Inhibitors	Virus titers ($\text{TCID}_{50}/\text{ml}$)	
	Inhibitor treatment during entry	Inhibitor treatment post entry
Control	6×10^4	6×10^4
0.45 M sucrose	2.5×10^4	0
2 mM MCD	1.9×10^4	n.d.
5 mM MCD	1.2×10^4	n.d.
25 μM chlorpromazine	3×10^3	0
20 mM NH_4Cl	3×10^4	1.2×10^2
50 μM CA074ME	2.4×10^4	1.2×10^2
20 μM CatLIII	1.8×10^4	0

Vero cells were infected with NiV at a MOI of 0.2. The inhibitors indicated were either added 1 h prior infection and during virus entry for 1 h at 37 °C (Inhibitor treatment *during entry*), or after removal of input virus at 1 h p.i. (Inhibitor treatment *post entry*). At 24 h p.i., virus titers in the cell supernatant were determined by the TCID_{50} method. n.d. = not done.

the proteolytic activation of newly synthesized F proteins, even if this endocytic pathway was found to be involved in EB2 and VLP uptake and might therefore play a role in receptor-mediated NiV uptake. When F protein cleavage was analyzed in the presence of 20 mM NH_4Cl , 20 μM E64d, a general cysteine protease inhibitor, 50 μM CA074ME, an inhibitor of cathepsin B and L (Montaser et al., 2002; Pager and Dutch, 2005), or 20 μM CatLIII, a CTSL-specific inhibitor, cleavage was found to be completely prevented (Fig. 3). This confirms that F activation in Vero cells depends on low pH and CTSL.

Drugs inhibiting endocytosis, acidification of the endosome or cathepsin-mediated cleavage do not affect NiV entry but later replication steps

To finally test if endocytic uptake and/or pH-dependent cathepsin-mediated processing within the endosomes are not only required for processing of newly synthesized F proteins but also for successful virus entry, NiV infections were carried out in the presence of the different inhibitors. In these infection experiments, the minimal, non-cytotoxic concentrations required for maximal cleavage inhibition determined before were used. All drugs and inhibitors were added to Vero cells 1 h prior

infection and were present during NiV infection at 37 °C. Because most of the infectious NiV had bound and entered the cells after 60 min and further incubation did not result in a more efficient infection (not shown), non-bound viruses and inhibitors were removed after 1 h of infection and cells were further cultured with serum-free medium. At 24 h post infection (p.i.), supernatants were taken for virus titration. To determine the amount of infected cells and to visualize syncytium formation, cells were immunostained using a polyclonal anti-NiV serum. As shown in Fig. 4A, NiV infection in untreated cells (control) induced extensive cell-to-cell fusion as indicated by the formation of large multinucleated syncytia. Interestingly, neither the addition of endocytosis inhibitors (0.45 M sucrose, 2 or 5 mM MCD, 25 μM chlorpromazine) nor treatment with 20 mM NH_4Cl , nor the addition of cathepsin B and L or CTSL-specific inhibitors (50 μM CA074ME; 20 μM CatLIII) had an effect on NiV infection. The amount and the size of syncytia were similar to those in the control infection, and also the virus titers in the cell supernatants did not substantially differ (Table 1, Inhibitor treatment *during entry*). As a control, Vero cells were infected with fowl plague virus (FPV) under the same conditions because it is well established that entry and fusion of influenza viruses absolutely depend on internalization and acidic pH within endosomes (Marsh and Helenius, 1989). The finding that FPV infection was drastically reduced when either endocytosis (0.45 M sucrose) or acidification of the endosome (20 mM NH_4Cl) was prevented clearly demonstrated that virus entry can be effectively hindered by the inhibitor treatments before and during virus adsorption (Fig. 5).

To analyze if the inhibitors have an effect if added after virus entry, Vero cells were infected with NiV for 1 h at 37 °C. After removal of non-bound viruses, cells were further incubated with serum-free medium containing the different inhibitors. Since MCD is highly toxic, it could not be used for longer incubation periods and was therefore not tested. At 24 h p.i., the outcome of the infection was again monitored by immunostaining of the infected cells and titration of the infectious virus in the supernatants. As shown in Fig. 4B, inhibitors disrupting endocytic uptake as well as inhibitors preventing cathepsin-mediated proteolytic processing drastically reduced syncytium formation. Release of infectious virions into the supernatant was also significantly decreased (Table 1, Inhibitor treatment *post entry*). To determine the number of initially infected cells in each

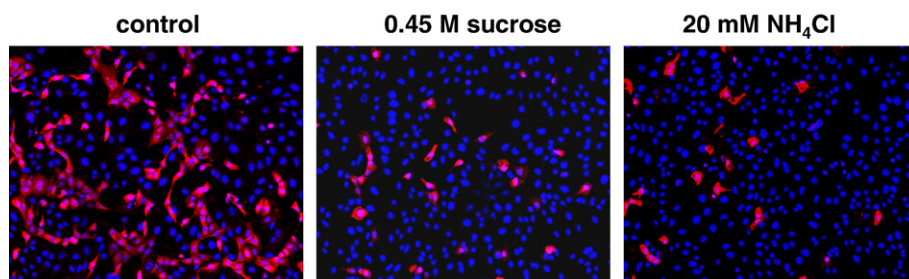


Fig. 5. Effect of sucrose and NH_4Cl treatment on influenza virus entry. Vero cells were infected with FPV at a MOI of 0.01. Cells were either left untreated (control) or incubated with the indicated inhibitors for 1 h prior infection and for 1 h during virus adsorption and entry. After washings to remove the inhibitors and input virus, residual virus attached to the cell surface was inactivated by acidic pH treatment. At 16 h p.i., cells were fixed and stained with a FPV-specific monoclonal antibody. Primary antibodies were detected with rhodamine-conjugated secondary antibodies and nuclei were visualized by DAPI staining.

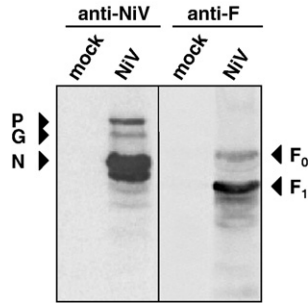


Fig. 6. F protein cleavage in purified NiV. Mock-sample and purified NiV were subjected to SDS-PAGE under reducing conditions and analyzed by Western blotting. Viral proteins were either detected with a polyclonal anti-NiV serum (anti-NiV) or with NiV F-specific antibodies (anti-F).

sample, NiV-positive single cells or syncytia (originating from one initially infected cell) in ten randomly chosen microscopic fields were counted and averaged. In mock-treated cells, we found an average of 2.5 syncytia per microscopic field (200× magnification). In inhibitor-treated cells, the mean number of single NiV-positive cells ranged from 2.0 to 2.8. Thus, the number of cells initially infected by NiV was very similar in all infections. This again indicates that inhibitor treatments did not interfere with virus entry and initial infection but solely prevented virus spread via cell-to-cell fusion and the release of infectious virus particles. Thus, endocytosis, acidic pH and cathepsin-mediated cleavage are not important for the initiation of a NiV infection in a new host cell but are only required during late stages of infection for the activation of newly synthesized F proteins.

Our findings imply that cell-free NiV particles contain sufficient amounts of cleaved F protein to be fully infectious. To check the amount of cleaved F protein in cell-free virions, we purified NiV from cell supernatants. The virus preparation was separated on a 12% SDS gel, blotted to nitrocellulose and either probed with a polyclonal anti-NiV serum recognizing predominantly the N, P and G protein, or incubated with an F-specific antiserum directed against the NiV F cytoplasmic tail, thus specifically detecting F₀ and F₁. The western blot analysis shown in Fig. 6 revealed that about 75% of the F protein in the virus preparation was cleaved. This clearly confirms that F cleavage occurs before incorporation into budding virions.

Discussion

The initial stages in infection of enveloped virions involve attachment to cell surface receptors followed by fusion with cellular membranes to release the viral nucleocapsids into the cytoplasm. Receptor binding and low pH are known to be the two main triggering mechanisms responsible for conformational changes in the viral glycoproteins leading to virus–cell fusion. For pH-independent viruses such as paramyxoviruses, structural changes in the fusion protein occur through interaction with the viral receptor (Lamb et al., 2006). For pH-dependent viruses such as toga-, rhabdo-, alpha-, flavi- and orthomyxoviruses, low pH triggers conformational changes in the fusion protein after

internalization into endosomes (Jardetzky and Lamb, 2004; Kielian and Rey, 2006). For endocytic uptake many different pathways are used by these viruses including macropinocytosis, phagocytosis, clathrin- and caveolae-mediated pathways and some less-well defined routes called non-clathrin-, non-caveolae-dependent pathways (Marsh and Helenius, 2006). An additional pH- and endocytosis-dependent entry strategy has been recently proposed for Ebola virus and SARS coronavirus (SARS-CoV). These viruses enter a new host cell via endocytosis followed by acid-dependent digestion by cathepsins to accomplish the fusion competence of the viral glycoproteins (Chandran et al., 2005; Kaletsky et al., 2007; Schornberg et al., 2006; Simmons et al., 2005).

At least for coronaviruses, it is known that members of the same virus family can use distinct pathways for fusion protein activation and virus entry. Whereas SARS-CoV and mouse hepatitis virus (MHV)-2 require uptake by endocytosis and subsequent proteolysis by cathepsins (Qiu et al., 2006; Simmons et al., 2005), infectious bronchitis virus only needs an acidification step (Chu et al., 2006) and the MHV-A59 strain or human CoV NL63 can enter the cell by pH-independent fusion at the plasma membrane (Huang et al., 2006; Qiu et al., 2006). The finding that the NiV F protein must be activated by endosomal proteases raised the possibility that NiV, similar to SARS-CoV, MHV-2 or Ebola virus, and in contrast to other paramyxoviruses, depends on pH- and CTSL-dependent mechanisms of entry. The idea that NiV can use other pathways than direct fusion at the plasma membrane was also encouraged by the recent report that Newcastle disease virus (NDV), a prototype member of the paramyxovirus family, can enter the cells via caveolae-mediated endocytosis (Cantin et al., 2007). Since EB2 is a raft- and thus caveolae-associated membrane protein (Gauthier and Robbins, 2003) and is furthermore constitutively internalized from the cell surface, NiV might enter caveosomes via receptor-mediated endocytosis. In support of this hypothesis, we found that EB2- and VLP uptake was affected by MCD, an inhibitor of caveolae-mediated endocytosis. However, MCD, sucrose or chlorpromazine treatment during virus entry had only a slight negative effect on productive virus infection. This indicates that none of the endocytic pathways is required during early virus replication steps. Consequently, acid-dependent endosomal F cleavage by CTSL cannot be a prerequisite for successful NiV entry. In agreement, addition of NH₄Cl or cathepsin inhibitors during early virus replication steps did not significantly reduce the infection. Even if these results do not rule out that endosomal entry pathways can be an alternative route of virus entry, they clearly show that post entry F processing in endosomes is not required for the infectivity of NiV. Similar to paramyxoviruses with furin-activatable F proteins such as measles or mumps virus, NiV F cleavage occurs before virus assembly and incorporation into budding virus particles.

In contrast to paramyxovirus F proteins which are activated by furin, most of the surface-expressed NiV F protein is uncleaved. Even if 60–70% of newly synthesized NiV F proteins are cleaved within 2 h in Vero cells (compare Fig. 3A), less than 10% of the protein found on the cell surface is proteolytically processed and fusion active (Moll et al., 2004a). This is very likely due to an

inefficient recycling to the plasma membrane after clathrin-mediated uptake and CTSL cleavage of endocytosed F proteins. Since paramyxovirus assembly is mainly directed by interactions of the matrix protein with the cytoplasmic or transmembrane portions of the viral glycoproteins (Peebles, 1991), proteolytic processing of the F ectodomain has no influence on the incorporation into budding particles. Thus, the content of cleaved F protein in cell-free virus particles directly depends on the amount of activated protein present in the cellular compartment where the assembly process has taken place. The fact that despite the low amounts of cleaved F proteins on the plasma membrane, fully infectious NiV particles containing about 75% of cleaved and fusion-active F proteins are released from infected cells might indicate that NiV assembly does not occur at the cell surface but at endosomal membranes. Fitting into this concept, the second NiV envelope glycoprotein, the G protein is also internalized from the cell surface (Vogt et al., 2005). The recent finding that the NiV M protein contains a late domain motif of the YxxL type known to interact with AP-2, a component of the clathrin-associated adaptor complex, and with AIP-1/ALIX, which functions in the formation of multivesicular bodies, a specialized endocytic compartment (Ciancanelli and Basler, 2006; Chen et al., 2005; Irie et al., 2007; Puffer et al., 1997), further supports the idea that endosomal compartments are not only involved in proteolytic activation of the F protein but might also be the site where all viral components are recruited for virus assembly.

Together, our results clearly demonstrate that despite internalization of both, the NiV receptor and NiV particles, endocytosis and a post entry cleavage mechanism are definitely not required for the NiV entry process. Even though the proteolytic activation of NiV F proteins clearly differs from other paramyxoviruses with respect to protease usage, CTSL, and the subcellular localization where cleavage takes place, endosomes, NiV particles released from infected cells contain sufficient amounts of cleaved and fusion-competent F proteins to initiate the infection of new host cells by pH-independent fusion with the plasma membrane.

Materials and methods

Cell culture and virus infection

Vero, 293T and HeLa cells were maintained in Dulbecco's modified minimal essential medium (DMEM; Gibco) supplemented with 10% fetal calf serum (FCS), 100 units/ml penicillin, and 0.1 mg/ml streptomycin. PAE (porcine aortic endothelial) cells were grown in DMEM/F12+GLUTAMAX (Gibco) supplemented with 10% FCS, penicillin and streptomycin. MDCK (Madin–Darby canine kidney) cells were propagated in MEM containing 10% FCS and antibiotics.

The NiV strain used in this study was isolated from human brain (kindly provided by J. Cardoso) and propagated as described previously (Moll et al., 2004a). For NiV infection studies, Vero cells were infected with NiV at a multiplicity of infection (MOI) of 0.2. After incubation for 1 h at 37 °C, virus was removed by extensive washings and cells were cultured with DMEM without FCS for 24 h at 37 °C. To prepare purified virus

for virus-uptake experiments and western blot analysis, Vero cells were infected with NiV at a MOI of 0.001. At 48 h post infection, supernatants were centrifuged at 4000 rpm for 10 min at 4 °C to remove cell debris and then pelleted through a 20% sucrose cushion at 28,000 rpm for 2 h at 4 °C in a SW28 Rotor (Beckman). After resuspending virus pellets in buffer containing 25 mM TRIS (pH 7.5), 150 mM NaCl and 5 mM EDTA (TNE) and a further centrifugation step at 35,000 rpm for 30 min at 4 °C in a SW41 Rotor (Beckman), concentrated and partially purified NiV was suspended in phosphate buffered saline (PBS) with 0.35% bovine serum albumin (BSA). All experiments with live NiV were performed under BSL4 conditions.

Plasmids and transfection

cDNA fragments spanning the G and the F genes of the NiV genome (GenBank™ accession number N° AF212302) were cloned into the pczCFG5 vector as described earlier (Moll et al., 2004b). To allow detection of the protein with commercially available antibodies, a tagged version of the proteins was established by inserting the amino acids YPYDVPDYA of the human influenza hemagglutinin (HA), known as HA-tag, at the C-terminus. Expression levels and biological activity of the HA-tagged proteins were unchanged compared to those of the parental F and G proteins in transient transfection. The human EB2 gene was kindly provided by D. Pfaff and H. Augustin and subcloned into the NotI and SacI restriction sites of the pCAGGS expression plasmid. Vero, MDCK, and HeLa cells were transfected by using the cationic lipid transfection reagent Lipofectamine 2000 (Invitrogen) following the instructions of the supplier. Stably EB2-expressing PAE cells were generated as described by Fuller et al. (2003) and kindly provided by H. Augustin.

Preparation of NiV G-containing virus-like particles (VLPs)

VLPs were generated as described by Wahl-Jensen et al. (2005). Briefly, 293T cells were transfected with a plasmid encoding NiV G_{tag} using the calcium phosphate transfection procedure (ProFection Mammalian Transfection System, Promega). At 72 h post transfection, supernatants were harvested, clarified from cellular debris by centrifugation at 3000 rpm for 15 min at 4 °C and then pelleted through a 20% sucrose cushion at 30,000 rpm for 2 h at 4 °C in a SW32 Rotor (Beckman). For washing, pellets were suspended in PBS and again centrifuged at 30,000 rpm for 40 min at 4 °C. Finally, VLP-containing pellets were resuspended in TNE containing 1% BSA and were stored at –20 °C. Each VLP preparation was controlled by electron microscopy and by western blot analysis using anti-HA-tag antibodies.

EB2 uptake assay

EB2-expressing cells were grown on cover slips to sub-confluency. Then, recombinant mouse EphB4/Fc, a soluble EB2 receptor fused to the Fc region of human IgG (R&D Systems) was added at a concentration of 2 µg/ml. After incubation for 1 h at 37 °C to allow binding and endocytosis to occur, surface-

remained EphB4/Fc was visualized with rhodamine-conjugated anti-human IgG antibodies (dilution 1:50; Jackson Immuno-Research) for 90 min at 4 °C. After fixation and permeabilization with methanol–acetone, internalized EphB4/Fc was stained by fluorescein isothiocyanate (FITC)-conjugated anti-human IgG antibodies (dilution 1:500; Dako) for 35 min at 4 °C. Fluorescence images were recorded using a Zeiss Axiovert 200M microscope.

Inhibitors

Endocytosis was inhibited by incubation with 0.45 M sucrose (Serva), 25 µM chlorpromazine (Sigma) or 5 mM β-methylcyclodextrin (MCD; Sigma). Acidification of the endosome was blocked by addition of 20 mM NH₄Cl (Sigma) and cathepsin-mediated proteolysis was prevented by the addition of either 20 µM E64d (Sigma), 20 µM CatLIII (Calbiochem) or 50 µM CA074ME (Sigma). All chemicals and drugs were dissolved in water or dimethylsulfoxide (E64d, CatLIII, CA074ME).

VLP uptake assay

Vero cells cultured on cover slips were pretreated with DMEM containing 2% FCS supplemented with 0.45 M sucrose, 25 µM chlorpromazine or 5 mM β-MCD for 30 min at 37 °C. Then, cells were incubated for 1 h at 37 °C with purified VLPs in combination with a monoclonal antibody directed against the HA-tag (dilution 1:200; Sigma) in the presence or absence of the inhibitors. As control, untreated cells were incubated for 1 h at 4 °C with VLPs and the antibody directed against the HA-tag. Surface-bound VLPs were stained by incubation with a FITC-conjugated anti-mouse IgG antibody (1:50; Jackson Immuno-Research) for 90 min at 4 °C. After fixation and permeabilization with methanol–acetone, intracellular VLPs were detected with a rhodamine-conjugated secondary antibody (1:500; Jackson ImmunoResearch) for 35 min at 4 °C. To visualize cell nuclei, 4',6'-diamidino-2-phenylindole (DAPI) was added to the secondary antibody. Representative images of merged of the DAPI, FITC and rhodamine channels were recorded with a Zeiss Axiovert 200M microscope.

NiV uptake assay

Vero cells grown on chamber slides (8well Permax[®] Slides; Nunc Lab-Tek) were incubated with purified NiV particles for 2 h at 4 °C. After addition of a polyclonal anti-NiV serum from an infected guinea pig (dilution 1:1000) for 30 min on ice, cells were washed several times to remove unbound virus and again incubated with anti-NiV guinea pig serum and then either shifted to 37 °C or kept at 4 °C for 20 min. Subsequently, surface-bound viruses were stained by incubation with FITC-conjugated anti-guinea pig antibodies (dilution 1:50; Jackson ImmunoResearch) for 1 h at 4 °C. After fixation and permeabilization with methanol–acetone, intracellular virus–antibody complexes were visualized with a rhodamine-conjugated secondary antibody (dilution of 1:300; Jackson ImmunoResearch) for 1 h at 4 °C and cell nuclei were stained as described before. Finally,

cells were incubated with 4% paraformaldehyde for 48 h and then, image recording was performed as described above.

Metabolic labeling and immunoprecipitation of the NiV F protein

To study the effect of the different drugs inhibiting endocytosis, acidification or cathepsins on NiV F protein cleavage, Vero cells were transfected with plasmid DNA encoding the NiV F gene. At 24 h post transfection, cells were incubated for 40 min with medium lacking cysteine and methionine (preincubation) followed by incubation with medium containing [³⁵S]-cysteine and -methionine (Promix, GE Healthcare) at a final concentration of 100 µCi for 10 min (pulse). Subsequently, labeling medium was replaced by serum-free medium for 2 h (chase). Inhibitors were present during preincubation, pulse and chase periods. After metabolic labeling, cells were lysed in radio-immunoprecipitation assay (RIPA) buffer (1% Triton X-100, 1% sodium deoxycholate, 0.1% SDS, 0.15 M NaCl, 10 mM EDTA, 10 mM iodoacetamide, 1 mM PMSF, 50 units/ml aprotinin, 20 mM Tris–HCl, pH 8.5) followed by centrifugation at 13,000 rpm for 30 min. NiV F protein was immunoprecipitated from cell lysates with the polyclonal anti-NiV serum at a final dilution of 1:500. After addition of 40 µl of a suspension of protein A-Sepharose (Sigma), immune complexes were washed three times with RIPA buffer, suspended in reducing sample buffer, and separated on a 12% polyacrylamide gel. Dried gels were exposed to autoradiography films (GE Healthcare).

Inhibitor studies with live NiV

To investigate the effect of inhibitors during different stages of infection, cells were left untreated (control) or were treated with the different chemicals or drugs inhibiting endocytosis, acidification or cathepsin cleavage. Inhibitors were either added 1 h before infection and for 1 h during virus adsorption and entry (Inhibitor treatment *during entry*) or were added 1 h after virus entry (Inhibitor treatment *after entry*). NiV infection was performed as described above. The amount of infected cells and syncytium formation were determined by indirect immunofluorescence. After fixation with 4% paraformaldehyde for 48 h and permeabilization with methanol–acetone, cells were incubated with the polyclonal guinea pig anti-NiV serum at a dilution of 1:1000 for 1 h at 4 °C. Primary antibodies were then detected with rhodamine-conjugated secondary antibodies (dilution 1:250). Images were recorded using a Zeiss AxioPhot microscope. Virus titers in the supernatant were determined by the 50% tissue culture infective dose (TCID₅₀) method on Vero cells (Reed and Muench, 1938).

Control infections with FPV

To control the effect of inhibitors on virus entry, Vero cells were left untreated or were treated with inhibitors for 1 h and then inoculated with influenza virus A/FPV/Rostock/34 (H7N1) (FPV) at a MOI of 0.01 in the absence or presence of the inhibitors for 1 h. After washings and inactivation of residual virus attached to

the cell surface with DMEM adjusted to pH 3 for 5 min, cells were further incubated at 37 °C. 16 h later, cells were fixed with methanol–acetone and FPV-infected cells were stained with a FPV-specific monoclonal antibody (HA1-2A11H7; kindly provided by W. Garten) at a dilution of 1:100 for 1 h at 4 °C. Primary antibodies were detected by incubation with rhodamine-conjugated secondary antibodies (dilution 1:200; Jackson Immuno-Research) and cell nuclei were visualized as described before. Representative images were recorded using a Zeiss Axiovert 200M microscope.

Western blot analysis of purified NiV

Concentrated and partially purified NiV was inactivated and disrupted in reducing sample buffer containing 1% SDS and subsequently heated for 10 min at 95 °C. Pelleted supernatants of mock infected Vero cells served as control. After separation on a 12% SDS gel, proteins were transferred to nitrocellulose. Non-specific binding sites were blocked by 5% nonfat dry milk in PBS. Blots were either incubated with polyclonal anti-NiV guinea pig serum (dilution 1:500) followed by incubation with horseradish peroxidase-conjugated rabbit anti-guinea pig immunoglobulin (dilution 1:2000; Dako), or were probed with a F-specific antibody directed against amino acids 523 to 541 of the NiV F cytoplasmic domain (dilution 1:200 in PBS; immunoGlobe Antikörpertechnik GmbH), followed by incubation with biotin-labeled anti-rabbit immunoglobulins (dilution 1:2000; Amersham) and horseradish peroxidase-conjugated streptavidin (dilution 1:2000; Amersham). Protein bands were visualized with the enhanced chemiluminescence system (SuperSignal® West Pico, Pierce) by exposure to an autoradiography film (GE Healthcare).

Acknowledgments

We thank M. Czub, S. Jones and H. Weingartl for supporting the BSL4 training of S.D. and for the NiV antibodies. We also thank D. Pfaff and H. Augustin for providing the EB2 gene and the EB2-expressing PAEC. This study was supported by the Deutsche Forschungsgemeinschaft to A.M. (DFG MA 1886/5-3 and SFB 593 TP B11). S.D. was supported by a fellowship from Boehringer Ingelheim.

References

- Adams, R.H., 2002. Vascular patterning by Eph receptor tyrosine kinases and ephrins. *Semin. Cell Dev. Biol.* 13, 55–60.
- Bonaparte, M.I., Dimitrov, A.S., Bossart, K.N., Cramer, G., Mungall, B.A., Bishop, K.A., Choudhry, V., Dimitrov, D.S., Wang, L.F., Eaton, B.T., Broder, C.C., 2005. Ephrin-B2 ligand is a functional receptor for Hendra virus and Nipah virus. *Proc. Natl. Acad. Sci. U. S. A.* 102, 10652–10657.
- Cantin, C., Holguera, J., Ferreira, L., Villar, E., Munoz-Barroso, I., 2007. Newcastle disease virus may enter cells by caveolae-mediated endocytosis. *J. Gen. Virol.* 88, 559–569.
- Chandran, K., Sullivan, N.J., Felbor, U., Whelan, S.P., Cunningham, J.M., 2005. Endosomal proteolysis of the Ebola virus glycoprotein is necessary for infection. *Science* 308, 1643–1645.
- Chen, C., Vincent, O., Jin, J., Weisz, O.A., Montelaro, R.C., 2005. Functions of early (AP-2) and late (AIP1/ALIX) endocytic proteins in equine infectious anemia virus budding. *J. Biol. Chem.* 280, 40474–40480.
- Chu, V.C., McElroy, L.J., Chu, V., Bauman, B.E., Whittaker, G.R., 2006. The avian coronavirus infectious bronchitis virus undergoes direct low-pH-dependent fusion activation during entry into host cells. *J. Virol.* 80, 3180–3188.
- Chua, K.B., 2003. Nipah virus outbreak in Malaysia. *J. Clin. Virol.* 26, 265–275.
- Ciancanelli, M.J., Basler, C.F., 2006. Mutation of YMYL in the Nipah virus matrix protein abrogates budding and alters subcellular localization. *J. Virol.* 80, 12070–12078.
- Diederich, S., Moll, M., Klenk, H.D., Maisner, A., 2005. The Nipah virus fusion protein is cleaved within the endosomal compartment. *J. Biol. Chem.* 280, 29899–29903.
- Earp, L.J., Delos, S.E., Park, H.E., White, J.M., 2005. The many mechanisms of viral membrane fusion proteins. *Curr. Top. Microbiol. Immunol.* 285, 25–66.
- Fuller, T., Korff, T., Kilian, A., Dandekar, G., Augustin, H.G., 2003. Forward EphB4 signaling in endothelial cells controls cellular repulsion and segregation from ephrinB2 positive cells. *J. Cell Sci.* 116, 2461–2470.
- Gauthier, L.R., Robbins, S.M., 2003. Ephrin signaling: one raft to rule them all? One raft to sort them? One raft to spread their call and in signaling bind them? *Life Sci.* 74, 207–216.
- Harcourt, B.H., Tamin, A., Ksiazek, T.G., Rollin, P.E., Anderson, L.J., Bellini, W.J., Rota, P.A., 2000. Molecular characterization of Nipah virus, a newly emergent paramyxovirus. *Virology* 271, 334–349.
- Huang, I.C., Bosch, B.J., Li, F., Li, W., Lee, K.H., Ghiran, S., Vasilieva, N., Dermody, T.S., Harrison, S.C., Dormitzer, P.R., Farzan, M., Rottier, P.J., Choe, H., 2006. SARS coronavirus, but not human coronavirus NL63, utilizes cathepsin L to infect ACE2-expressing cells. *J. Biol. Chem.* 281, 3198–3203.
- Irie, T., Shimazu, Y., Yoshida, T., Sakaguchi, T., 2007. The YLDL sequence within Sendai virus M protein is critical for budding of virus-like particles and interacts with Alix/AIP1 independently of C protein. *J. Virol.* 81, 2263–2273.
- Jardetzky, T.S., Lamb, R.A., 2004. Virology: a class act. *Nature* 427, 307–308.
- Kaletsky, R.L., Simmons, G., Bates, P., 2007. Proteolysis of the Ebola virus glycoproteins enhances virus binding and infectivity. *J. Virol.* 81, 13378–13384.
- Kielian, M., Rey, F.A., 2006. Virus membrane-fusion proteins: more than one way to make a hairpin. *Nat. Rev. Microbiol.* 4, 67–76.
- Klenk, H.D., Garten, W., 1994. Activation cleavage of viral spike proteins by host proteases. *Cellular Receptors for Animal Viruses*. Cold Spring Harbor Laboratory, Cold Spring Harbor, New York, pp. 241–280.
- Korff, T., Dandekar, G., Pfaff, D., Fuller, T., Goettsch, W., Morawietz, H., Schaffner, F., Augustin, H.G., 2006. Endothelial ephrinB2 is controlled by microenvironmental determinants and associates context-dependently with CD31. *Arterioscler. Thromb. Vasc. Biol.* 26, 468–474.
- Kullander, K., Klein, R., 2002. Mechanisms and functions of Eph and ephrin signalling. *Nat. Rev., Mol. Cell Biol.* 3, 475–486.
- Lamb, R.A., Paterson, R.G., Jardetzky, T.S., 2006. Paramyxovirus membrane fusion: lessons from the F and HN atomic structures. *Virology* 344, 30–37.
- Marsh, M., Helenius, A., 1989. Virus entry into animal cells. *Adv. Virus Res.* 36, 107–151.
- Marsh, M., Helenius, A., 2006. Virus entry: open sesame. *Cell* 124, 729–740.
- Meulendyke, K.A., Wurth, M.A., McCann, R.O., Dutch, R.E., 2005. Endocytosis plays a critical role in proteolytic processing of the Hendra virus fusion protein. *J. Virol.* 79, 12643–12649.
- Moll, M., Diederich, S., Klenk, H.D., Czub, M., Maisner, A., 2004a. Ubiquitous activation of the Nipah virus fusion protein does not require a basic amino acid at the cleavage site. *J. Virol.* 78, 9705–9712.
- Moll, M., Kaufmann, A., Maisner, A., 2004b. Influence of N-glycans on processing and biological activity of the nipah virus fusion protein. *J. Virol.* 78, 7274–7278.
- Montaser, M., Lalmanach, G., Mach, L., 2002. CA-074, but not its methyl ester CA-074Me, is a selective inhibitor of cathepsin B within living cells. *Biol. Chem.* 383, 1305–1308.
- Negrete, O.A., Levrony, E.L., Aguilar, H.C., Bertolotti-Ciarlet, A., Nazarian, R., Tajyar, S., Lee, B., 2005. EphrinB2 is the entry receptor for Nipah virus, an emergent deadly paramyxovirus. *Nature* 436, 401–405.

- Pager, C.T., Craft Jr., W.W., Patch, J., Dutch, R.E., 2006. A mature and fusogenic form of the Nipah virus fusion protein requires proteolytic processing by cathepsin L. *Virology* 346, 251–257.
- Pager, C.T., Dutch, R.E., 2005. Cathepsin L is involved in proteolytic processing of the Hendra virus fusion protein. *J. Virol.* 79, 12714–12720.
- Patch, J.R., Cramer, G., Wang, L.F., Eaton, B.T., Broder, C.C., 2007. Quantitative analysis of Nipah virus proteins released as virus-like particles reveals central role for the matrix protein. *Virol. J.* 4, 1–14.
- Peebles, M.E., 1991. Paramyxovirus M proteins. Pulling it all together and taking it on the road. *The Paramyxoviruses*. Plenum Press, New York, pp. 427–456.
- Puffer, B.A., Parent, L.J., Wills, J.W., Montelaro, R.C., 1997. Equine infectious anemia virus utilizes a YXXL motif within the late assembly domain of the Gag p9 protein. *J. Virol.* 71, 6541–6546.
- Qiu, Z., Hingley, S.T., Simmons, G., Yu, C., Das Sarma, J., Bates, P., Weiss, S.R., 2006. Endosomal proteolysis by cathepsins is necessary for murine coronavirus mouse hepatitis virus type 2 spike-mediated entry. *J. Virol.* 80, 5768–5776.
- Reed, L.J., Muench, H., 1938. A simple method of estimating fifty per cent endpoints. *J. Hyg.* 27, 493–497.
- Schornberg, K., Matsuyama, S., Kabsch, K., Delos, S., Bouton, A., White, J., 2006. Role of endosomal cathepsins in entry mediated by the Ebola virus glycoprotein. *J. Virol.* 80, 4174–4178.
- Simmons, G., Gosalia, D.N., Rennekamp, A.J., Reeves, J.D., Diamond, S.L., Bates, P., 2005. Inhibitors of cathepsin L prevent severe acute respiratory syndrome coronavirus entry. *Proc. Natl. Acad. Sci. U. S. A.* 102, 11876–11881.
- Vogt, C., Eickmann, M., Diederich, S., Moll, M., Maisner, A., 2005. Endocytosis of the nipah virus glycoproteins. *J. Virol.* 79, 3865–3872.
- Wahl-Jensen, V.M., Afanasieva, T.A., Seebach, J., Stroher, U., Feldmann, H., Schnittler, H.J., 2005. Effects of Ebola virus glycoproteins on endothelial cell activation and barrier function. *J. Virol.* 79, 10442–10450.
- Wang, L.F., Yu, M., Hansson, E., Pritchard, L.I., Shiell, B., Michalski, W.P., Eaton, B.T., 2000. The exceptionally large genome of Hendra virus: support for creation of a new genus within the family *Paramyxoviridae*. *J. Virol.* 74, 9972–9979.
- Wong, K.T., Shieh, W.J., Kumar, S., Norain, K., Abdullah, W., Guarner, J., Goldsmith, C.S., Chua, K.B., Lam, S.K., Tan, C.T., Goh, K.J., Chong, H.T., Jusoh, R., Rollin, P.E., Ksiazek, T.G., Zaki, S.R., 2002. Nipah virus infection: pathology and pathogenesis of an emerging paramyxoviral zoonosis. *Am. J. Pathol.* 161, 2153–2167.
- Yob, J.M., Field, H., Rashdi, A.M., Morrissy, C., van der Heide, B., Rota, P., bin Adzhar, A., White, J., Daniels, P., Jamaluddin, A., Ksiazek, T., 2001. Nipah virus infection in bats (order Chiroptera) in peninsular Malaysia. *Emerg. Infect. Dis.* 7, 439–441.